Review Article

Plasma characteristics and dynamics in a high power pulsed magnetron sputtering discharge[*]

XIA Yuan[†]   GAO Fangyuan   LI Guang

(*Institute of Mechanics, Chinese Academy of Sciences, Beijing 100190, China*)

Xia Y, Gao F Y, Li G. Plasma characteristics and dynamics in a high power pulsed magnetron sputtering discharge[J]. Journal of University of Chinese Academy of Sciences, 2015, 32(2): 145-154.

Abstract   High power impulse magnetron sputtering (HIPIMS) is a promising technology that has drawn attention in both academia and industry in recent years. HIPIMS, also known as high power pulse magnetron sputtering, is a physical vapor deposition technique. The high power has been brought to extremely high discharge current density of several $A \cdot cm^{-2}$ and HIPIMS has been successfully developed to produce high plasma densities of the order of 10^{19} m^{-3}. The plasma properties in sputtering process have shown the great advantages, which make it possible to control the deposition process and optimize the performance of films. In this paper, we show the I-V characteristics of discharge and the design of power supply, as well as the ionization rate of sputtered atoms. Furthermore, the spatial and the temporal evolution of plasma, the non-normal transport of ionized species, and the deposition rate are reviewed.

Key words   HIPIMS; HPPMS; plasma dynamics; discharge characteristic; high ionization rate

CLC Number: TB43   **Document code**: A   **doi**: 10.7523/j.issn.2095-6134.2015.02.001

高功率脉冲磁控溅射放电的等离子体特性与动力学

夏源 高芳源 李光

(中国科学院力学研究所, 北京 100190)

摘要 高功率脉冲磁控溅射(HIPIMS)是近年来在学术界和工业界备受关注的一项技术. HIPIMS又称高功率脉冲磁控溅射(HPPMS). 通过采用极高的放电电流密度(几个 $A \cdot cm^{-2}$; 可以成功获得高密度的等离子体(密度可达 10^{19} m^{-3}. 溅射过程中等离子体的特性显示出独特的优势, 使得控制沉积过程和优化薄膜性能成为可能. 本文综述了HIPIMS放电的IV特性和电源设计、溅射原子的电离率、等离子体时空演化、离子的非正常输运以及沉积速率等.

关键词 高功率脉冲磁控溅射; 高功率脉冲磁控溅射; 等离子体动力学; 放电特性; 高电离率

.

HIPIMS; HPPMS;   ;   ;

Magnetron sputtering as a well-established physical vapor deposition (PVD) technique has been used to deposit different coatings for a wide range of applications. Because of the ability to be easily controlled by electric and magnetic fields the charged particles such as ions are advantageous for facilitating plasma-ion processing. Therefore the efficient production of charged particles is indispensable for current PVD techniques. High power impulse magnetron sputtering (HIPIMS) is a promising technique for ion assisted film growth and surface engineering by which nearly full ionization of the sputtered Ti atoms has been obtained [1] . The method was introduced by Kouznetsov et al. [2]   and has drawn attention in both academia and industry in recent years [3-4] .

In HIPIMS the high power leads to peak electron densities exceeding 10^{19} m^{-3} in the positions close to targets which are three times higher than those achieved by conventional sputtering techniques [5-6] . The high density of electron increases the ionization impact probability between sputtered atom and high energy electron therefore high ionization sputtering material particles are gained. Through the control of electric and magnetic fields the charged particles can obtain higher ion energy. It is precisely the reason that HIPIMS has been successfully developed to obtain high-quality films with high adhesion high density and good corrosion resistance and wear resistance. This technique has been demonstrated to be useful for substrate cleaning high-aspect-ratio filling application and improvement of microstructure of thin films [1 2 7-10] .

Many studies [11-14] indicate that plasma environment has a significant impact on structure and properties of the films in deposition process. Therefore to better control the film growth process to find the optimal experimental conditions and to obtain high quality thin films further study of the plasma characteristics and transport dynamics is necessary. Great attention has been paid to the unique plasma properties in sputtering process with the developement of HIPIMS. Extensive investigations have shown the outstanding advantages of HIPIMS compared with other magnetron sputtering techniques from the initial electron density [5 15] to the recent distribution of ion energy [16-18] . In the following sections the typical characteristics and dynamics of plasma in HIPIMS will be discussed to clarify its illustrious excellences in industrial applications.

1 *I–V* characteristics of gas discharge in HIPIMS

As early as in 1903 Townsend explained the mechanism of gas discharge using the concept of gas ionization namely the Townsend theory. The discharge characteristic curve of low pressure gas is shown in Fig. 1 and the curre is mainly divided into normal glow discharge abnormal glow discharge and arc discharge pant. Studies showed that the *I–V* characteristics of conventional DC magnetron sputtering (dcMS) are mainly located in the early stage of abnormal glow discharge while those of cathodic arc (CA) are located in the stage of arc discharge. In fact the exploration of HIPIMS has filled the gap between the dcMS and the CA. The *I–V* characteristic curves of HIPIMS meet the back-end of abnormal glow discharge region and therefore are more difficult to control as the instability.
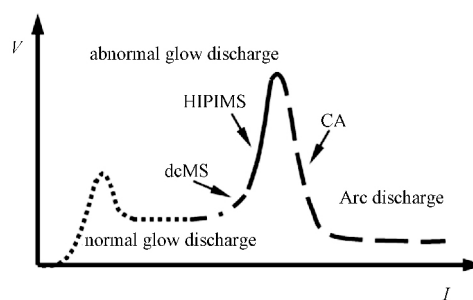

Fig. 1 Discharge characteristic curve of low pressure gas

In DC magnetron sputtering the target current I_d and the target voltage V_d follow a certain functional relation: $I_d = K_d V_d^{\,n}$ [19]   where K_d is a constant. The exponent n is typically within the range of 5 ~ 15 which mainly depends on the target material type magnetic field and other experimental parameters. In HIPIMS there is also a similar function between the peak target current density and the target voltage. Figure 2 shows the target voltage versus the peak target current density for a conventional DC magnetron sputtering discharge and a HIPIMS discharge respectively [20]. For the conventional DC magnetron sputtering the exponent n is approximately 8. The HIPIMS discharge exhibits two slopes depending on the target current. For the low current density region the exponent n is about 7 indicating the conventional magnetron sputtering discharge mode. At higher current density the exponent n is suddenly reduced to 1 which is well consistent with the Townsend curve. Alami et al. [21] have carried out the similar research about the sudden change in discharge pattern. This sudden increase in the resistance of discharge has been considered to be caused by a sharp reduced capture of secondary electrons [20].
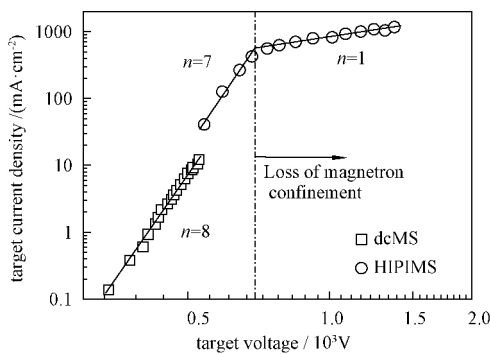

Fig. 2   Target voltage versus peak target current density for a magnetron in dcMS and HIPIMS modes respectively [20]

2　Plasma characteristics in HIPIMS

2.1　High discharge current density

For conventional magnetron sputtering the maximum power is limited because of the thermal load on the target provided by the bombardment of positive ions. To avoid this limitation high-power pulsed magnetron sputtering introduced a method by making a lower duty cycle（on-time divided by the cycle-time） while a corresponding increase in power during the on-time. This not only has resolved the thermal load problem but also brought the peak discharge current density to the order of several $A\cdot cm^{-2}$ [1,2,20]. HIPIMS power is mainly based on single or multiple LC circuit networks [22-24]. The voltage and current waveform is determined not only by the power supply but also by the load such as magnetron sputtering device magnetic field structure target material gas type and pressure of the vacuum chamber [5,25-29].

Figure 3 shows how the pulse shapes depend on the argon pressure [5]. It can be seen that the plasma ignition point has a close relationship with the gas pressure. With the increase of gas pressure the pulse duration decreased and the plasma ionization could be achieved instantly without time delay in the case of low pressure. To solve the problem of time delay the plasma is pre-ionized by a DC power supply in some of the high power pulse systems [8,30-32].
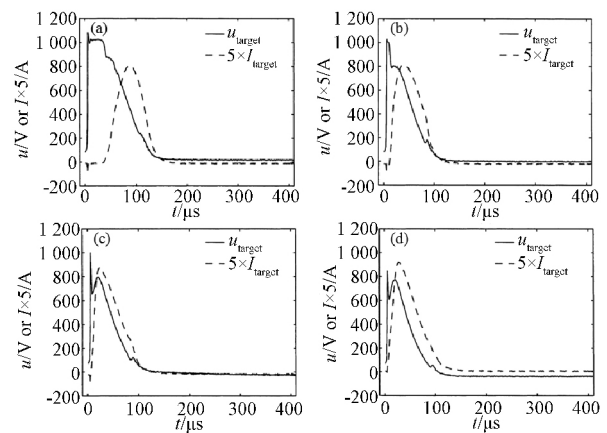

Fig. 3   Target current and voltage waveform produced by the HIPIMS power supply at working pressures of （a）0.06 Pa （b）0.26 Pa （c）1.33 Pa and（d）2.66 Pa [5]

2.2　High ionization rate

Compared with the conventional magnetron sputtering methods in which the ions available are mainly the ions of the inert sputtering gas a high degree of ionization of the sputtered atoms is a

significant feature for HIPIMS. Optical emission spectroscopy （OES） studies have confirmed an enhanced proportion of ions of both residual gas and sputtered species in the HIPIMS discharge [7 20 32-34] . Figure 4 shows the typical OES spectra from HIPIMS and conventional magnetron sputtering discharges of Cr in Ar at the same average power [7] . Strong emission from Cr ions is observed in the HIPIMS plasma both singly and doubly ionized while the ratio of Cr ion to neutral spectral line is negligible in the conventional magnetron sputtering. As a result the ionization rate increased significantly and the ionized flux fraction for Cr had been estimated to be roughly 30% by the weight gain method.
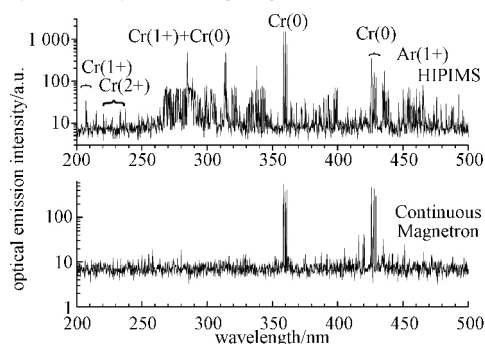

Fig. 4   Typical OES spectra for the plasma composition in HIPIMS and conventional magnetron sputtering of Cr in Ar atmosphere at the same average power [7]

Konstantinidis et al. [33] showed that the ionization rate is higher than 50% for a Ti target and increases with increasing applied power and pulse length. Bohlmark et al. [34] also observed the ion contribution of the sputtered Ti increases with increasing applied pulse energy and reaches values higher than 90%. The ion-to-neutral ratios as a function of the peak target current of the sputtered Cr are shown in Fig. 5 [20] . The diagnostic results indicate an increased ion-to-neutral ratios of Cr^{2+}/Cr^0 and Cr^{1+}/Cr^0 with target current. It can be also concluded that the degree of ionization is very high for Cr. Bohlmark et al. [32] showed that the ion flux contained more metal ions （Ti^{1+} 50% Ti^{2+} 24%） than inert gas ions （Ar^{1+} 23% Ar^{2+} 3%） during the intense moment of the discharge. The peak Ti^{1+}/Ar^{1+} ratio is over two. Therefore the HIPIMS discharge
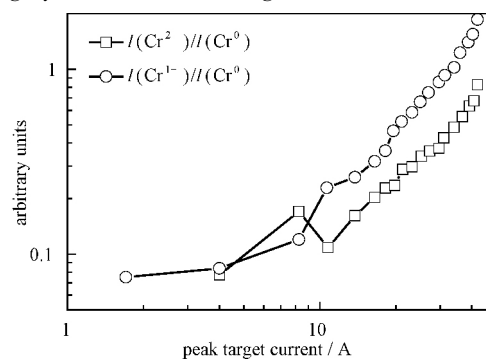
is highly metallic containing.

Fig. 5   Ion-to-neutral ratio as a function of the peak target current for Cr from optical emission line intensities [20]

2. 3   High ion energy distribution

It is well known that the trajectory can be changed in an $E \times B$ drift loop only for the charged particles. The high degree of ionization creates new opportunities since the ions can be controlled by using electric or magnetic fields and obtain higher ion energy. The ion energy distribution function （IEDF） for an HIPIMS and a dcMS discharges are shown in Fig. 6 [32] . There are distinct differences in the energy distribution observed for the two techniques. For HIPIMS the ion energy distribution is broader extending to a more intense high-energy tail 100 eV. The energy of about 50% of the Ti ions is higher than 20 eV. Similar results have been observed by Erkens et al. [35] and Lin et al. [36] .
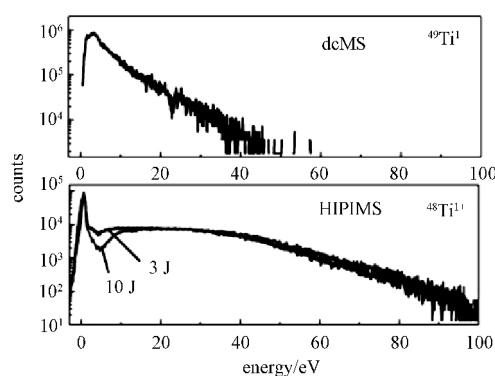

Fig. 6   Ion energy distributions for Ti^{1+} ions measured in dcMS and HIPIMS discharges [32]

Due to the large fraction of energetic ions produced by HIPIMS the technique provides high-quality films with excellent adhesion high density and smooth surfaces. The energetic ions can serve as

effective adhesion promoters for momentum transfer and film densification during film growth. Figure 7 shows the chemical composition profile of the CrN coating in which the substrate was pretreated by HIPIMS with the negative voltage of 1 200 V [7] . A transition region with a width of approximately 40 nm is confirmed while Cr increases and Fe decreases. It can be considered that Cr is implanted in the stainless steel substrates. An incorporation of 4 at.% of Ar is characterized at the interface which is a result of the high energy gas/metal ion etching [37] . This process was shown to enhance the adhesion with values of LC up to 85 N [7] . The microstructure of interfaces pretreated by HIPIMS of Cr is shown in Fig. 8 [38] . The interface is clean and dense which appears to be a clear boundary owing to the intensive bombardment by high fractions of metal ions. Therefore the presence of high-energy

Fig. 7   STEM-EDS analysis of the chemical composition at the coating-substrate interface after pretreatment and CrN coating deposition by HIPIMS [7]

Fig. 8   Cross sectional views of the interface between the CrN base layer and the stainless steel substrate pretreated by HIPIMS with $U_{bias} = -1\,000$ V [38]

ions is significant for the improvements in coating adhesion structure and properties.

3   Plasma dynamics in HIPIMS

In the process of film growth the plasma conditions across the chamber have a significant impact on the performance of films. Better mapping of the plasma dynamics is therefore necessary to fix process parameters and optimize preparations for films in an HIPIMS system. The following text will be divided into three stages occurrence transport and deposition to describe the research results on plasma dynamics in HIPIMS.

3.1   Occurrence

The discharge characteristics of HIPIMS have been studied by Anders et al. [26] . The discharge consists of two phases. The first phase can be ascribed to argon ions and secondary electrons generated by them and the immediately followed second stage depends on the sustained self-sputtering which can provide high power. The self-sputter-dominated phase not only strongly depends on the material but also the correlation with the secondary electrons. The yield of secondary electrons strongly depends on the potential energy of the primary ions and the generation of charged metal ions is critical for the maintenance of the self-sputter dominated phase. Self-sputter yields for various target materials as a function of primary ion kinetic energy is shown in Fig. 9 [26] . It can be seen that carbon has a very small sputter yield and thus it can not go in the self-sputter dominated mode. Other materials all have the self-sputter dominated phase in their own pronounced manner.

The ionization mechanism in an HIPIMS discharge has been reported [39] . The results show that a large number of electrons are trapped in the magnetic field near the targets during the pulse-on period and the most effective process in creating metal ions is the electron impact ionization. After the pulse is off charge exchange becomes the dominant process in ionization of metal atoms.
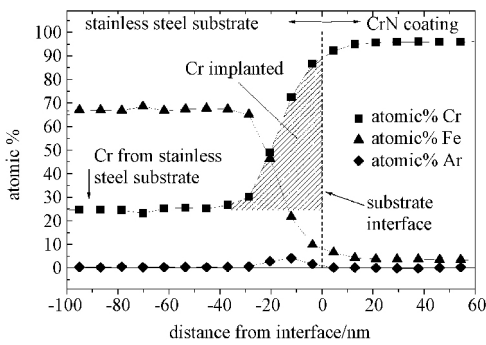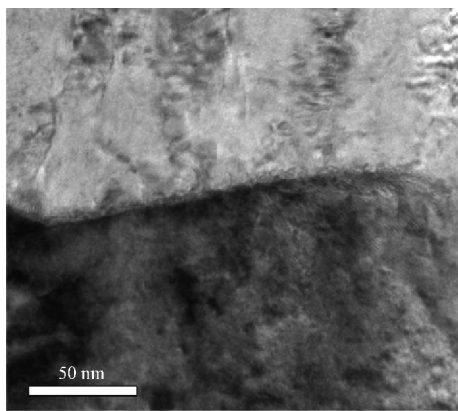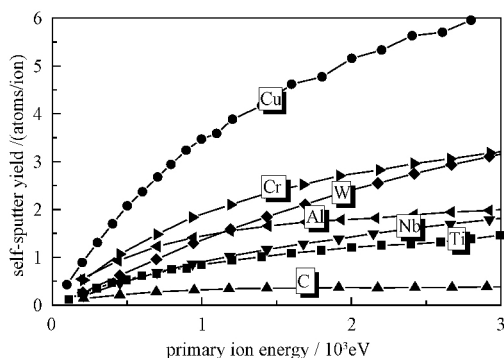
Fig. 9 SRIM-calculated self-sputter yields as functions of primary ion kinetic energy for various target materials [26]

3.2 Transport

The spatial and temporal variation in the plasma parameters such as electron density average electron energy plasma potential and electron energy distribution function (EEDF) can be calculated from I–V curves obtained by Langmuir probes [2 5 15 20]. Gudmundsson et al. [5] have observed the time-dependent electron density for different pressures and distances away from the target cathode. The peak electron density is in the range of $(2-8) \times 10^{18}$ m^{-3} and decreases with the decreasing inert gas pressure or the increasing distance. The spatial and temporal evolution of the electron density in a plane perpendicular to the surface of the magnetron has been explored by Bohlmark et al. [40]. A high-density doughnut shaped plasma forms above the race track in the early stage of the discharge. It demonstrates how the high density plasma expands away from the target surface. The trajectories of the peak intensity of the expanding plasma at three different Ar pressures are shown in Fig. 10 [5]. This peak travels away from the target with a fixed velocity which decreases with increasing operating pressure. A best fit through the data gives the traveling velocity of the electron density peak of 4.0×10^5 cm/s at 0.06 Pa 1.8×10^5 cm/s at 0.26 Pa and 0.8×10^5 cm/s at 1.33 Pa.

The evolution of the electron energy distribution function (EEDF) with time from initiating the pulse has been reported [15 41]. According to the measured

I–V characteristics of a Langmuir probe the EEDF is determined using the Druyvesteyn formula [42-43]. Initially the distribution can be described by a single peak indicating a Druyvesteyn like. Towards the end of the pulse two energy groups of electrons are present. With the disappearance of the high-energy electron group the electron energy distribution appears to be Maxwellian like. Eventually the plasma becomes more Druyvesteyn like with lower electron density and higher average electron energy.
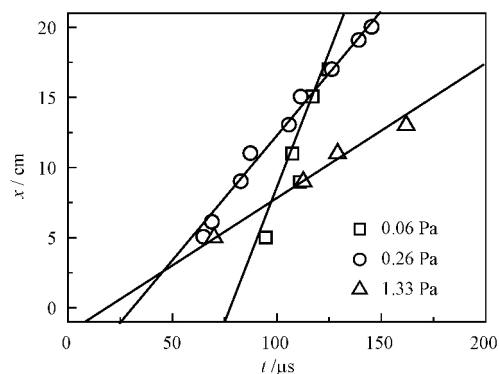

Fig. 10 Trajectory of the peak intensity of the expanding plasma at different Ar pressures [5]

The temporal behavior of the plasma density was influenced by the process conditions such as sputtering gas chamber dimension distance to target and applied power [25]. The time evolution has also been measured for the ion species in the plasma [44-45]. Figure 11 shows the integrals of the ion energy distribution function as a measure of the number of ions entering the mass spectrometer [46].
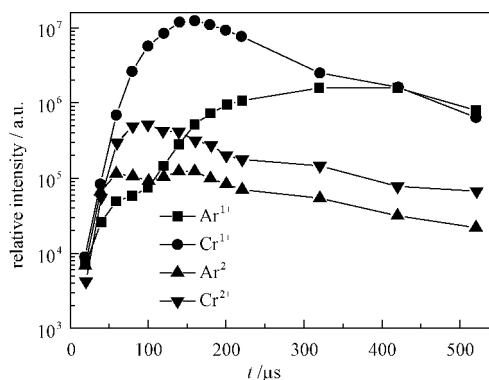

Fig. 11 Integrals of the IEDF in HIPIMS plasma discharge with Cr target [46]

Since the start of the pulse the Cr^{1+} flux dominates the value until 420 μs when more Ar^{1+} ions are detected. The peak of the Cr^{1+} ion flux has been ten times the peak of the Ar^{1+} ions. The Ar^{2+} ion flux seems to have two extrema the first one coming with metal ions and the second one coming with the Ar^{1+} flux. The first wave could be due to the energy transferred from sputtering particles to nearby gas particles while the second wave could originate from the particles near the target region.

Measured with the thermal probe facing the magnetron surface the energy flux distribution in an HIPIMS plasma of approximate 500 W average power is presented in Fig. 12 [47]   while the previous investigations on energy flux have been mainly focused on the axial flux [48]. It is indicated that the heat flux increases towards the surface of the magnetron and peaks in the region between the race track ($\rho = 4.5$ cm) and the rim of the magnetron. Compared with the centre at $\rho = 0$ cm the energy flux is as twice large as at $\rho = 8$ cm in the near–cathode region ($z = 4$ cm). The energy flux profile shows more homogeneously distributed away from the cathode surface and the radial variation of the energy flux is rather small at $z > 10$ cm.
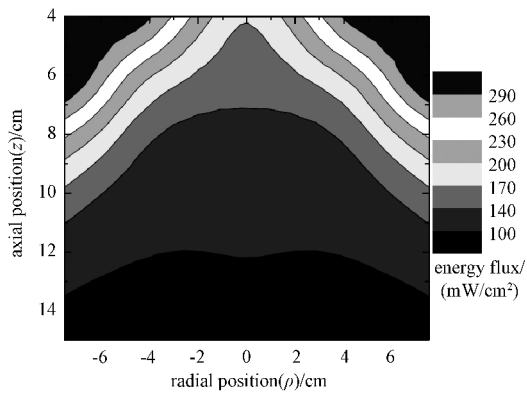

Fig. 12   Energy flux distribution at the radial (ρ) and axial (z) by HIPIMS at average power of 500 W [47]

3. 3   Deposition

Compared to the atoms the high–energy ions are provided with better diffraction gain in electromagnetic field and thus the films prepared by HIPIMS greatly improve the uniformity and flatness [49-50]. The technology is widely used for high–aspect–ratio filling and high–quality films preparation. However in the HIPIMS discharge the deposition rate is found to be generally lower than in a conventional dcMS discharge for an equivalent amount of power [51-55]. Konstantinidis et al. [54] found the effect of the pulse on/off time configuration on the deposition rate of films grown by HIPIMS and as the pulse length decreases from 20 μs to 5 μs for the same average power the deposition rate increases from 20% to 70% of dcMS values. Figure 13 shows the obtained deposition rates for dcMS and HIPIMS by using an equal average power with different inclination angles of the substrates [55]. When samples grown facing the target surface ($\theta = 0°$) the deposition rate for HIPIMS is approximately 40% in DC sputtering. However it is seen that the deposition rate of dcMS suffers from a significantly larger decrease than HIPIMS for substrates placed at a large angle ($\theta > 90°$). For HIPIMS films grown at the inclination angle of 90° the deposition rate dropped to about 42% of the value measured at the inclination angle of 0° while the corresponding values for dcMS reduced to 17% as demonstrated. The results further reflect that the plasma in HIPIMS possesses better diffraction.
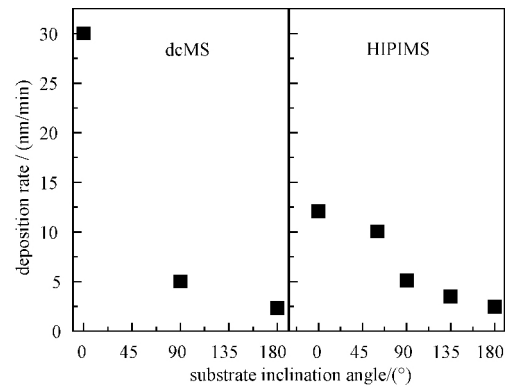

Fig. 13   Normalized deposition rates measured for films grown by dcMS and HIPIMS at different inclination angles [55]

The decreased deposition rate in HIPIMS has been explained mainly by the fact that the ions can be attracted back toward the target and captured by the cathode potential [56]. The reduction is expected

to occur especially for metals with a low self-sputtering yield. The deposition efficiency for HIPIMS compared with a dcMS discharge plotted as a function of the metals self-sputtering yield divided by its Ar-sputter yield is developed by Christie [53]. Some other possible explanations for the reduction in deposition rate in HIPIMS are due to the low conductivity or magnetic confinement in the target-to-substrate region [54-57]. Recent results show that the deposition rate can be optimized by placing an rf-driven inductively coupled discharge [58] or applying a magnetic coil [59] between the target and the substrate. Therefore the problem of a lower deposition rate can be solved through a number of methods.

4 Expectation

The studies on plasma dynamics in HIPIMS process have been reviewed. The main emphasis in this work was placed on the newly developed PVD technique which provides high power densities high ionization fraction and high ion energy distribution. With the outstanding advantages the technique already plays an important role in various coating applications such as conformal growth of films on non-flat substrates substrate pre-treatment for improved adhesion and preparation of high-performance thin films.

So far several groups not only studied the physical properties of plasma but also showed solicitude for the relationship between experimental parameters and film structures [60-62]. However the researches lack the discussion about their intermediate "plasma" which is crucial for increasing film production in the stability and repeatability. Therefore the development trend in future will be by studying and interpreting the secrets of "plasma" to achieve the relationships among experimental parameters plasma and film structures and to provide the basis for the realization of industrial production.

References

1 Bohlmark J Alami J Christou C et al. Ionization of sputtered metals in high power pulsed magnetron sputtering J . J Vac Sci Technol A Vac Surf Films 2005 23(1): 18-23.

2 Kouznetsov V Macǎk K Schneider J M et al. A novel pulsed magnetron sputter technique utilizing very high target power densities J . Surf Coat Technol 1999 122(2/3): 290-293.

3 Sarakinos K Alami J Konstantinidis S. High power pulsed magnetron sputtering: a review on scientific and engineering state of the art J . Surf Coat Technol 2010 204 (11): 1 661-1 684.

4 Gudmundsson J T Brenning N Lundin D et al. High power impulse magnetron sputtering discharge J . J Vac Sci Technol A 2012 30(3): 030 801-18.

5 Gudmundsson J T Alami J Helmersson U. Spatial and temporal behavior of the plasma parameters in a pulsed magnetron discharge J . Surf Coat Technol 2002 161(2/3): 249-256.

6 Bohlmark J Gudmundsson J T Alami J et al. Spatial electron density distribution in a high-power pulsed magnetron discharge J . IEEE Trans Plasma Sci 2005 33 (2): 346-347.

7 Ehiasarian A P Münz W D Hultman L et al. High power pulsed magnetron sputtered CrNx films J . Surf Coat Technol 2003 163-164: 267-272.

8 Vǎsina P Měsko M Ganciu M et al. Reduction of transient regime in fast preionized high-power pulsed-magnetron discharge J . Europhys Lett 2005 72(3): 390-395.

9 Alami J Eklund P Emmerlich J et al. High-power impulse magnetron sputtering of Ti-Si-C thin films from a Ti$_3$SiC$_2$ compound target J . Thin Solid Films 2006 515 (4): 1 731-1 736.

10 Reinhard C Ehiasarian A P Hovsepian P Eh. CrN/NbN superlattice structured coatings with enhanced corrosion resistance achieved by high power impulse magnetron sputtering interface pre-treatment J . Thin Solid Films 2007 515(7/8): 3 685-3 692.

11 Anders A Ni P Rauch A. Drifting localization of ionization runaway: Unraveling the nature of anomalous transport in high power impulse magnetron sputtering J . J Appl Phys 2012 111(5): 053 304-13.

12 Anders A. Self-organization and self-limitation in high power impulse magnetron sputtering J . Appl Phys Lett 2012 100(22): 224 104-5.

13 Ehiasarian A P Hecimovic A Arcos T de los et al. High power impulse magnetron sputtering discharges: instabilities

and plasma self-organization J . Appl Phys Lett 2012 100
（11）：114 101-4.

14 Kozyrev A V Sochugov N S Oskomov K V et al. Optical
studies of plasma inhomogeneities in a high-current pulsed
magnetron discharge J . Plasma Phys Rep 2011 37（7）：
621-627.

15 Gudmundsson J T Alami J Helmersson U. Evolution of the
electron energy distribution and plasma parameters in a pulsed
magnetron discharge J . Appl Phys Lett 2001 78（22）：
3 427-3 429.

16 Lin J Moore J J Sproul W D et al. Ion energy and mass
distributions of the plasma during modulated pulse power
magnetron sputtering J . Surf Coat Technol 2009 203
（24）：3 676-3 685.

17 Oks E M Anders A. Boron-rich plasma by high power
impulse magnetron sputtering of lanthanum hexaboride J . J
Appl Phys 2012 112（8）：086 103-3.

18 Bowes M Poolcharuansin P Bradley J W. Negative ion
energy distributions in reactive HiPIMS J . J Phys D:
Applm Phys 2013 46（4）：045 204-9.

19 Rossnagel S M Kaufman H R. Current voltage relations in
magnetrons J . J Vac Sci Technol A 1988 6（2）：
223-229.

20 Ehiasarian A P New R Münz W D et al. Influence of high
power densities on the composition of pulsed magnetron
plasmas J . Vacuum 2002 65（2）：147-154.

21 Alami J Sarakinos K Mark G et al. On the deposition rate
in a high power pulsed magnetron sputtering discharge J .
Appl Phys Lett 2006 89（15）：154 104-3.

22 Kouznetzov V. Method and apparatus for magnetically
enhanced sputtering P . US Patent 2001 US 6296742 B1.

23 Sproul W D Christie D J Carter D C et al. Pulsed plasma
for sputtering applications J . Surf Eng 2004 20（3）：174-
180.

24 Christie D J Tomasel F Sproul W D et al. Power supply
with arc handling for high peak power magnetron sputtering
 J . J Vac Sci Technol A Vac Surf Films 2004 22（4）：
1 415-1 419.

25 Alami J Gudmundsson J T Bohlmark J et al. Plasma
dynamics in a highly ionized pulsed magnetron discharge J .
Plasma Sources Sci Technol 2005 14（3）：525-531.

26 Anders A Andersson J Ehiasarian A. High power impulse
magnetron sputtering: current-voltage-time characteristics
indicate the onset of sustained self-sputtering J . J Appl
Phys 2007 102（11）：113 303-11.

27 Yukimura K Mieda R Azuma K et al. Voltage-current
characteristics of a high-power pulsed sputtering（HPPS）
glow discharge and plasma density estimation J . Nucl
Instrum Methods Phys Res B 2009 267（8/9）：1 692-

1 695.

28 Benzeggouta D Hugon M C Bretagne J et al. Study of a
HPPMS discharge in Ar/O$_2$ mixture: I. Discharge
characteristics with Ru cathode J . Plasma Sources Sci
Technol 2009 18（4）：045 025-9.

29 Nakano T Hirukawa N Saeki S et al. Effects of target
voltage during pulse-off period in pulsed magnetron sputtering
on afterglow plasma and deposited film structure J .
Vacuum 2013 87：109-113.

30 Bugaev S P Sochugov N S. Production of large-area coatings
on glasses and plastics J . Surf Coat Technol 2000 131（1
-3）：474-480.

31 Chistyakov R. Plasma source for semiconductor manufacturing
industry e. g. plasma etching has power supply to generate
electric field ionizing volume of feed gas and another supply
generating another field super-ionizing initial plasma P .
World Patent 2004 WO 2004/095 497 A2.

32 Bohlmark J Lattemann M Gudmundsson J T et al. The ion
energy distributions and ion flux composition from a high
power impulse magnetron sputtering discharge J . Thin Solid
Films 2006 515（4）：1 522-1 526.

33 Konstantinidis S Dauchot J P Ganciu M et al. Influence of
pulse duration on the plasma characteristics in high-power
pulsed magnetron discharges J . J Appl Phys 2006 99
（1）：013 307-5.

34 Bohlmark J Alami J Christou C et al. Ionization of
sputtered metals in high power pulsed magnetron sputtering
 J . J Vac Sci Technol A Vac Surf Films 2005 23（1）：
18-22.

35 Erkens G Cremer R Hamoudi T et al. Properties and
performance of high aluminum containing（Ti Al）N based
supernitride coatings in innovative cutting applications J .
Surf Coat Technol 2004 177-178：727-734.

36 Lin J Moore J J Sproul W D et al. Ion energy and mass
distributions of the plasma during modulated pulse power
magnetron sputtering J . Surf Coat Technol 2009 203
（24）：3 676-3 685.

37 Sch önjahn C Ehiasarian A P Lewis D B et al.
Optimization of in situ substrate surface treatment in a
cathodic arc plasma: a study by TEM and plasma diagnostics
 J . J Vac Sci Technol A 2001 19（4）：1 415-1 420.

38 Ehiasariana A P Wen J G Petrov I. Interface microstructure
engineering by high power impulse magnetron sputtering for
the enhancement of adhesion J . J Appl Phys 2007 101
（5）：054 301-10.

39 Gudmundsson J T. Ionization mechanism in the high power
impulse magnetron sputtering（HiPIMS）discharge J . J
Phys 2008 100：082 013-4.

40 Bohlmark J Gudmundsson J T Alami J et al. Spatial

electron density distribution in a high-power pulsed magnetron discharge J . IEEE Trans Plasma Sci 2005 33 (2): 346-347.

41 Stranak V Herrendorf A P Drache S et al. Plasma diagnostics of low pressure high power impulse magnetron sputtering assisted by electron cyclotron wave resonance plasma J . J Appl Phys 2012 112(9): 093 305-9.

42 Druyvesteyn M J. The low arc volt J . Z Phys 1930 64 (11 /12): 781-798.

43 Lieberman M A Lichtenberg A J. Principles of Plasma Discharges and Materials Processing M . 2nd ed Wiley New York. 2005: 191.

44 Hecimovic A Arcos T de los Schulz-von der Gathen V et al. Temporal evolution of the radial plasma emissivity profile in HIPIMS plasma discharges J . Plasma Sources Sci Technol 2012 21(3): 035 017-9.

45 Aiempanakit M Aijaz A Lundin D et al. Understanding the discharge current behavior in reactive high power impulse magnetron sputtering of oxides J . J Appl Phys 2013 113 (13): 133 302-8.

46 Hecimovic A Ehiasarian A P. Time evolution of ion energies in HIPIMS of chromium plasma discharge J . J Phys D: Appl Phys 2009 42(13): 135 209-9.

47 Lundin D Stahl M Kersten H et al. Energy flux measurements in high power impulse magnetron sputtering J . J Phys D: Appl Phys 2009 42(18): 185 202-7.

48 Rohde D Berndt J Deutsch H et al. Investigations on the energy influx at plasma processes by means of a simple thermal probe J . Thin Solid Films 2000 377-378: 585-591.

49 Alami J Persson P O Å Music D et al. Ion-assisted physical vapor deposition for enhanced film properties on nonflat surfaces J . J Vac Sci Technol A 2005 23 (2): 278-280.

50 Bobzin K Bagcivan N Immich P et al. Mechanical properties and oxidation behaviour of (Al Cr) N and (Al Cr Si) N coatings for cutting tools deposited by HPPMS J . Thin Solid Films 2008 517(3): 1 251-1 256.

51 Sproul W D Christie D J Carter D C et al. Pulsed plasmas foil sputtering applications J . Surf Eng 2004 20 (3): 174-176.

52 Vl? ek J Pajdarová A D Musil J. Pulsed dc magnetron discharges and their utilization in plasma surface engineering J . Contrib Plasma Phys 2004 44(5 /6): 426-436.

53 Christie D J. Target material pathways model for high power pulsed magnetron sputtering J . J Vac Sci Technol A Vac Surf Films 2005 23(2): 330-335.

54 Konstantinidis S Dauchot J P Ganciu M et al. Influence of pulse duration on the plasma characteristics in high-power pulsed magnetron discharges J . J Appl Phys 2006 99 (1): 013 307-5.

55 Alami J Eklund P Andersson J M et al. Phase tailoring of Ta thin films by highly ionized pulsed magnetron sputtering J . Thin Solid Films 2007 515(7 /8): 3 434-3 438.

56 Hosokawa N Tsukada T Kitahara H. Preparation and properties of carbon-films with magnetron sputtering R . Proceedings of the 8th International Vacuum Congress 1980 Cannes France 1: 115-116.

57 Bugaev S P Koval N N Sochugov N S et al. Investigation of a high-current pulsed magnetron discharge initiated in the low-pressure diffuse arc plasma C ∥Proceedings of the 17th International Symposium on Discharges and Electrical Insulation in Vacuum 1996 Berkeley CA USA 1/2: 1 074-1 076.

58 Konstantinidis S Dauchot J P Ganciu M et al. Transport of ionized metal atoms in high-power pulsed magnetron discharges assisted by inductively coupled plasma J . Appl Phys Lett 2006 88(2): 021 501-3.

59 Bohlmark J Östbye M Lattemann M et al. Guiding the deposition flux in an ionized magnetron discharge J . Thin Solid Films 2006 515(4): 1 928-1 931.

60 Alami J Sarakinos K Uslu F et al. On the relationship between the peak target current and the morphology of chromium nitride thin films deposited by reactive high power pulsed magnetron sputtering J . J Phys D: Appl Phys 2009 42(1): 015 304-7.

61 Bagcivan N Bobzin K Theiß S. ($Cr_{1-x} Al_x$) N: a comparison of direct current middle frequency pulsed and high power pulsed magnetron sputtering for injection molding components J . Thin Solid Films 2013 528: 180-186.

62 Partridge J G Mayes E L H McDougall N L et al. Characterization and device applications of ZnO films deposited by high power impulse magnetron sputtering (HiPIMS) J . J Phys D: Appl Phys 2013 46 (16): 165 105-5.